Polymer Chemistry

ROYAL SOCIETY OF CHEMISTRY

COMMUNICATION

View Article Online
View Journal | View Issue

Open Access Article. Published on 07 June 2022. Downloaded on 12/30/2025 1:10:31 PM.
This article is licensed under a Creative Commons Attribution 3.0 Unported Licence.

Check for updates

Cite this: *Polym. Chem.*, 2022, **13**, 3750

Received 25th April 2022,
Accepted 6th June 2022

DOI: 10.1039/d2py00530a

rsc.li/polymers

RAFT dispersion polymerization induced self-assembly (PISA) of boronic acid-substituted acrylamides†

Harpal S. Dhiraj, [a] Fumi Ishizuka, [b] Amr Elshaer, [a] Per B. Zetterlund *[b] and Fawaz Aldabbagh *[a]

Reversible addition–fragmentation chain transfer (RAFT)-mediated dispersion polymerization induced self-assembly (PISA) of boronic acid (BA)-substituted acrylamides is established. The first PISA on unprotected BA-substituted monomer yields spherical nanoparticles (NPs) that undergo room-temperature transitions to higher order morphologies upon dilution with the dispersion solvent. PISA with the BA pinacol ester-derivative yields spherical NPs, worms, and vesicles.

Boronic acid (BA) is a Lewis acid moiety utilized in analytical and biomedical applications, most notably sugar sensing.[1,2] Polymerization induced self-assembly (PISA) allows direct access to high concentrations of block copolymer core–shell nanoparticles (NPs) without polymer processing.[3–6] The most widely used reversible deactivation radical polymerization (RDRP) or controlled/living technique for PISA is reversible addition–fragmentation chain transfer (RAFT) polymerization.[6] For PISA of BA-substituted monomers, only a pinacol ester-protected BA acrylate and methacrylate are reported (Scheme 1(a)(i and ii)).[7,8] RAFT-mediated PISA of 4-pinacolboronylbenzyl methacrylate (BBMA) was implemented as an emulsion polymerization in water/EtOH and dispersion polymerization in methanol (MeOH).[7] The dispersion polymerization involved chain extension of poly(oligo(ethylene glycol) methacrylate) (POEGMA) macroRAFT agents with BBMA to give sub-100 nm spheres at high conversion. Hsu and Delaittre *et al.* proposed applications in boron-neutron capture therapy[9] for BA pinacol-ester derivative NPs.[7] Fan and Thang *et al.* reported the dispersion polymerization of the acrylate analogue also in MeOH, using poly(DMA, *N*,*N*-dimethylacrylamide) macroRAFT agents as the steric stabilizer block.[8] In this case, a range of higher order polymer objects were achieved, including with

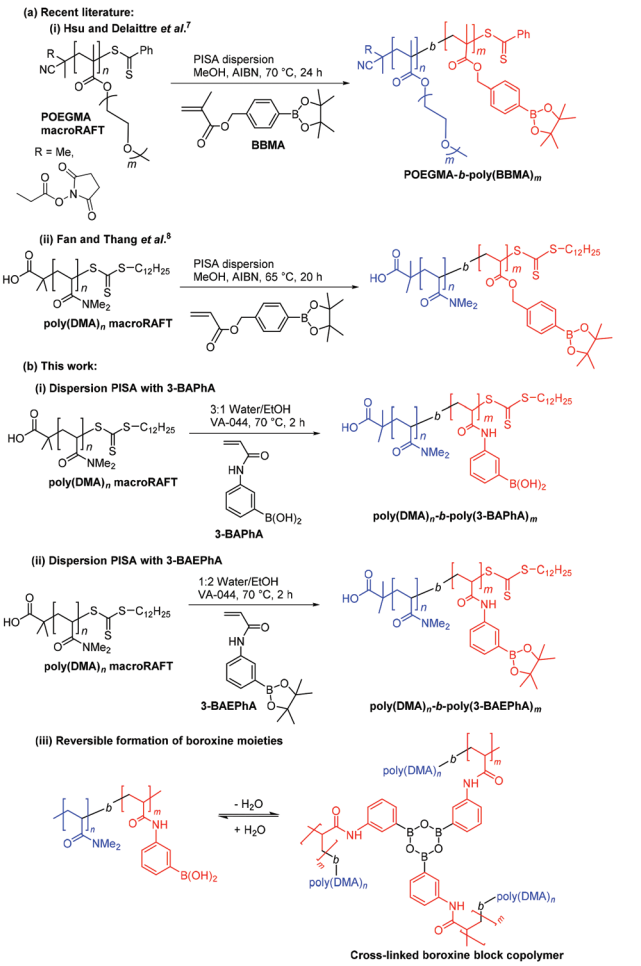

Scheme 1 PISA of BA, BA-pinacol ester protected monomers and equilibrium for boroxine formation.

[a]*Department of Pharmacy, School of Life Sciences, Pharmacy and Chemistry, Kingston University, Penrhyn Road, Kingston upon Thames, KT1 2EE, UK. E-mail: f.aldabbagh@kingston.ac.uk*

[b]*Cluster for Advanced Macromolecular Design (CAMD), School of Chemical Engineering, The University of New South Wales, Sydney, NSW 2052, Australia. E-mail: p.zetterlund@unsw.edu.au*

†Electronic supplementary information (ESI) available: Experimental section, additional figs, including TEMs and NMR spectra. See DOI: https://doi.org/10.1039/d2py00530a

This journal is © The Royal Society of Chemistry 2022

Open Access Article. Published on 07 June 2022. Downloaded on 12/30/2025 1:10:31 PM.
This article is licensed under a Creative Commons Attribution 3.0 Unported Licence.

cubic and hexagonal mesophases, and oxidative removal of the BA group led to disassembly.

Sumerlin *et al.* pioneered controlled/living homogeneous polymerizations of BA-substituted phenylacrylamides (PhAs).[2,10–12] Polymerization of (3-acrylamidophenyl)boronic acid (3-BAPhA) in DMF-5% water at 70 °C used 2-(dodecylthiocarbonothioylthio)-2-methylpropionic acid (DMP) and 2,2′-azobisisobutyronitrile (AIBN) as the RAFT agent and azo initiator, respectively.[10] The polymerizations displayed controlled/living characteristics with M_n of 37 800 g mol^{-1} and $Đ$ of 1.16 at $[3\text{-BAPhA}]_0/[DMP]_0$ = 200. The polymerization of BA-substituted monomers can however be challenging due to dehydration giving boroxine cross-linked chains.[13,14] There is also the requirement for pinacol protection of the BA moieties prior to GPC analysis.[10,11,13] This led to RAFT-mediated polymerization using the pinacol ester protected (3-acrylamidophenyl)boronic acid (3-BAEPhA) monomer in DMF at 70 °C.[12] Control was demonstrated by linear increases in M_n up to 68–74% conversion in accordance with reaction stoichiometry for $[3\text{-BAEPhA}]_0/[DMP]_0$ = 100 and $[3\text{-BAEPhA}]_0/[DMP]_0$ = 200. Chain extension with hydrophilic DMA or *N*-isopropylacrylamide (NIPAM) gave sugar and thermally-responsive block copolymer micelles after dialysis of the block copolymer solutions with water.[10–12] This traditional block copolymer self-assembly method is however time-consuming and results in low concentrations of NPs (<1% wt/vol%).[15] Dialysis involves the reduction in the solvency of the hydrophobic poly(3-BAPhA) block by slow exchange of the organic solvent with water.

In the present study, we use dispersion polymerizations of 3-BAPhA or 3-BAEPhA monomer (20 wt/vol%) from hydrophilic poly(DMA) macroRAFT agents to establish high concentrations of BA-functionalized amphiphilic (all) polyacrylamide core–shell NPs (Scheme 1(b)(i and ii)). We have thus carried out the first PISA on an unprotected BA-substituted monomer, and PISA with the pinacol ester derivative allowed the attainment of higher order macro-objects.

The water-soluble azo initiator 2,2′-azobis[2-(2-imidazolin-2-yl)propane]dihydrochloride (VA-044) was chosen due to its high decomposition rate coefficient (k_d) allowing completion of each polymerization in 2 h at 70 °C while maximizing livingness.[16] Solution homopolymerizations using VA-044 and the RAFT agent DMP and the monomers DMA and 3-BAPhA gave solvophilic poly(DMA) macroRAFT agents,[17] (for subsequent chain extensions) and poly(3-BAPhA) for solubility studies (see ESI†), respectively. 3-BAPhA and the derived homopolymer are soluble in hot water, but to meet the requirements for dispersion polymerization, the polymer needs to be insoluble. This was achieved through the addition of ethanol with 3 : 1 water/EtOH, providing soluble monomer and insoluble poly(3-BAPhA) at 70 °C.

Initial studies involved optimizing the initiator concentration ($[VA\text{-}044]_0$) for the 2 h dispersion polymerization of 3-BAPhA (20 wt/vol%) using poly$(DMA)_{28}$ as macroRAFT agent at 70 °C. Three different initiator concentrations at $[\text{poly}(DMA)_{28}]_0/[VA\text{-}044]_0$ = 70, 57 and 45 were investigated, at a targeted degree of polymerization of $[3\text{-BAPhA}]_0/[\text{poly}(DMA)_{28}]_0$ = 50 (Fig. 1). For the lowest $[VA\text{-}044]_0$, the solution remained transparent and conversion was low (23%, Run 1; Table 1), with the low rate of polymerization (R_P) attributed to the absence of particle nucleation. After nucleation, monomer swell the formed micelles, leading to a relatively high local monomer concentration, and thus rate enhancement.[18,19]

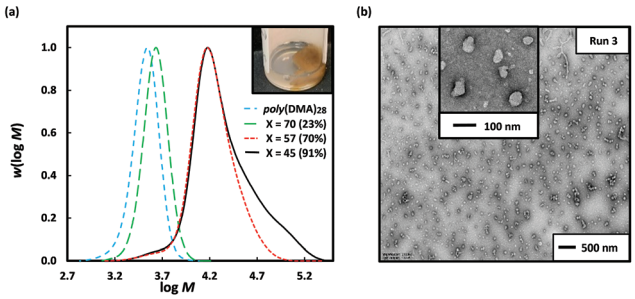

Fig. 1 Varying the initiator concentration $[VA\text{-}044]_0$ for the 2 h RAFT dispersion polymerization of 3-BAPhA (20 wt/vol%) in 3 : 1 water/EtOH at 70 °C using $[3\text{-BAPhA}]_0/[\text{poly}(DMA)_{28}]_0$ = 50, with $[\text{poly}(DMA)_{28}]_0/[VA\text{-}044]_0$ = X (Run 1–3). (a) MWDs after pinacol protection (with conv.) and visual appearance of polymerization for X = 45; (b) TEM images for PISA at X = 45 (additional images in Fig. S1†).

Considerably higher conversion (70%) was obtained for $[\text{poly}(DMA)_{28}]_0/[VA\text{-}044]_0$ = 57, with relatively good control/livingness (M_n = 14 600 g mol^{-1}; $M_{n,th}$ = 12 700 g mol^{-1}; $Đ$ = 1.35) (Run 2, Table 1). Note that the GPC data are recorded after the pinacol-protection of BA moieties to give poly(3-BAEPhA) and is subject to calibration error against linear polystyrene standards. Near-complete conversion (91%, Run 3) was obtained at the highest VA-044 concentration, but with a broad molecular weight distribution (MWD, $Đ$ = 1.80), with M_n (19 500 g mol^{-1}) higher than $M_{n,th}$ (15 700 g mol^{-1}). The two polymerizations of 3-BAPhA at high conversions led to significant agglomeration, which visibly increases upon cooling. This brown coagulum is assumed to be boroxine, which is the anhydride of BA formed in the solid state,[20] and is in equilibrium in solution (Scheme 1(b)(iii)).[14] Boroxine is favored at the locus of polymerization (within the monomer-rich particles), where the concentration of water is low, in contrast to the dispersion medium. Part of the highest conversion sample (Run 3) could however be re-suspended on shaking, with TEM analysis indicating irregularly shaped near-spherical sub-100 nm solid particles (Fig. 1).

Attempts to circumvent the formation of coagulum by carrying out the dispersion polymerization of 3-BAPhA using poly$(DMA)_{28}$ macroRAFT at lower monomer loadings resulted in low R_P, agglomeration and inferior control/living character. The use of a longer hydrophilic macroRAFT agent was investigated – this would lead to a significant delay in the on-set of particle nucleation, but the longer stabiliser block may improve colloidal stability. Thus dispersion polymerization of 3-BAPhA (20 wt/vol%) was carried out using poly$(DMA)_{96}$ macroRAFT agent (as opposed to poly$(DMA)_{28}$); a free-flowing colloidal dispersion formed, as indicated by a cloudy-white

Open Access Article. Published on 07 June 2022. Downloaded on 12/30/2025 1:10:31 PM.
This article is licensed under a Creative Commons Attribution 3.0 Unported Licence.

Table 1 Experimental results for dispersion PISA of 3-BAPhA and 3-BAEPhA using poly(DMA) macroRAFT agents (Scheme 1b(i and ii))

Run[a]	$[M]_0/[\text{poly(DMA)}]_0$	Polymer[b]	Conv.[c] (%)	$M_{n,th}$[d]	M_n[e]	$Đ$	Vis.[g]	TEM[h]
1	50	Poly(DMA)_{28}-*b*-$\text{poly(3-BAPhA)}_{12}$	23	6400	4000[f]	1.10[f]	sol	—
2	50	Poly(DMA)_{28}-*b*-$\text{poly(3-BAPhA)}_{35}$	70	12 700	14 600[f]	1.35[f]	cg	—
3	50	Poly(DMA)_{28}-*b*-$\text{poly(3-BAPhA)}_{46}$	91	15 700	19 500[f]	1.80[f]	cg&dis	s
4	50	Poly(DMA)_{96}-*b*-$\text{poly(3-BAPhA)}_{50}$	99	23 600	24 500[f]	1.27[f]	cg&dis	s
5	50	Poly(DMA)_{96}-*b*-$\text{poly(3-BAEPhA)}_{50}$	99	23 600	20 700	1.57	gel	w
6	150	Poly(DMA)_{96}-*b*-$\text{poly(3-BAEPhA)}_{149}$	99	50 600	39 000	1.76	gel	s
7	200	Poly(DMA)_{96}-*b*-$\text{poly(3-BAEPhA)}_{198}$	99	64 000	44 500	1.76	gel	s
8	50	Poly(DMA)_{36}-*b*-$\text{poly(3-BAEPhA)}_{50}$	99	17 600	23 600	1.15	gel	s
9	100	Poly(DMA)_{36}-*b*-$\text{poly(3-BAEPhA)}_{99}$	99	30 900	30 500	1.28	dis	v
10	150	Poly(DMA)_{36}-*b*-$\text{poly(3-BAEPhA)}_{149}$	99	44 600	43 100	1.38	dis	v
11	200	Poly(DMA)_{36}-*b*-$\text{poly(3-BAEPhA)}_{198}$	99	58 000	40 800	1.63	dis	v

[a] See Fig. 1–4 for dispersion polymerization conditions and conversions. [b] DP of the stabilizer block is calculated from M_n(GPC) poly(DMA)_{28} (3100 g mol^{-1}, $Đ$ = 1.12), poly(DMA)_{96} (9900 g mol^{-1}, $Đ$ = 1.17) and poly(DMA)_{36} (3900 g mol^{-1}, $Đ$ = 1.10), and the DP of the poly(3-BAPhA) and poly(3-BAEPhA) block is based on conversion. [c] Measured by ^{1}H NMR, see ESI.† [d] Theoretical ($M_{n,th}$) is calculated from poly(3-BAEPhA) DP added to the poly(DMA) M_n(GPC). [e] g mol^{-1} and determined by GPC/RI in DMF (0.01 M LiBr). [f] GPC for the polymerization of 3-BAPhA is after pinacol protection to poly(3-BAEPhA) (see ESI†). [g] Visual appearance, where sol, cg, and dis are solution, coagulum, and dispersion respectively. [h] Major morphology, where s, w, and v are spheres, worms, and vesicles respectively.

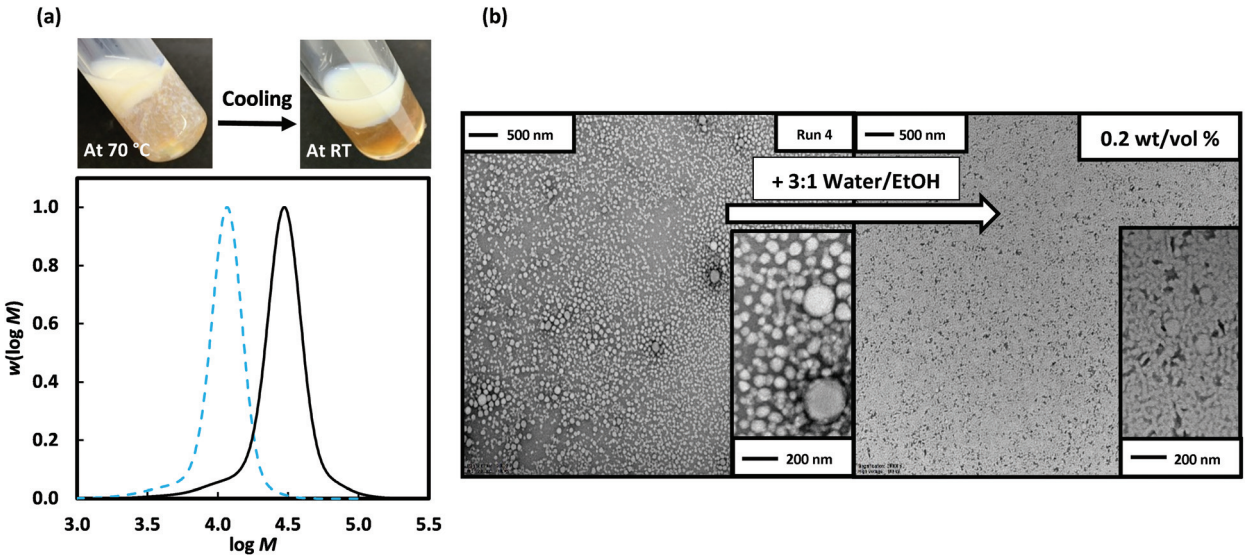

Fig. 2 Poly(DMA)_{96}, as macroRAFT agent (dashed blue line) in the 2 h dispersion polymerizations of 3-BAPhA (20 wt/vol%; full black line) in 3 : 1 water/EtOH at 70 °C, where $[\text{poly(DMA)}_{96}]_0/[\text{VA-044}]_0$ = 40, and targeted degree of polymerization, DP = 50 (Run 4). (a) Visual appearance of polymerization (with white stirrer bar within) before and after cooling to RT, and MWD (99% conv.) after pinacol protection; (b) TEM images for PISA after separation of the cooled cloudy dispersion (upper layer) and room temp (RT) dilution 100-fold with 3 : 1 water/EtOH (same as polymerization medium, TEM after 24 h) (additional images in Fig. S3 and S4,† respectively).

layer, which separated from the lower brown agglomeration upon cooling (Fig. 2). The polymerization reached completion (99% conv., Run 4), with excellent control/living character demonstrated by M_n (24 500 g mol^{-1}) in close agreement with $M_{n,th}$ (23 600 g mol^{-1}), and a narrow MWD ($Đ$ = 1.27) (Table 1). The MWD of the upper colloidal layer was superimposable with that of the lower brown coagulum (Fig. S2†), indicating that boroxine formation had not affected control/livingness. TEM analysis of the white dispersion layer showed mainly small spherical NPs (Fig. 2(b)), but with some short rods, and large well-defined up to 200 nm spherical particles. Given the distinct possibility of boroxine moieties (Scheme 1(b)(iii)), colloidal stability was evaluated through 100-fold dilution with the dispersion solvent (3 : 1 water/EtOH) at room temp. After 24 h, TEM analysis for the dilution showed the primary morphology was short rods and worms with some similar sized 50–100 nm diameters spheres remaining (Fig. 2). A lesser (20-fold) dilution of the upper layer with the dispersion solvent (at room temp.), after 24 h, gave a greater abundance of spheres compared to rods, reflecting less boroxine hydrolysis (Fig. S5†). A decrease in polymer concentration would normally reduce the likelihood of transitions to higher order morphologies, since the number of polymer aggregates and thus collisions is less.[21] However, in this case, increased hydrolysis

 This journal is © The Royal Society of Chemistry 2022

Open Access Article. Published on 07 June 2022. Downloaded on 12/30/2025 1:10:31 PM.
This article is licensed under a Creative Commons Attribution 3.0 Unported Licence.

of boroxine at the core shifts the equilibrium from crosslinked polymer to linear poly(BA) chains, so affecting the interfacial energy and consequently self-assembly. This change in hydrophilic–hydrophobic block and polymer-solvent interactions is presumed to cause the observed sphere-to-rod (worm) transition.

To circumvent boroxine, pinacol-protected BA (3-BAEPhA) was investigated. Homogeneous (solution) RAFT-mediated polymerizations of 3-BAPhA and 3-BAEPhA (1 M) using AIBN and DMP at 70 °C proceeded with almost identical R_P and similar control/living character indicated by overlapping points on the conversion *vs.* time and M_n *versus* conversion plots (Fig. S6†). However, the 3-BAPhA polymerization MWDs were consistently broader ($Đ$ = 1.48–1.61) than for the pinacol derivative ($Đ$ = 1.31–1.45), possibly due to the presence of boroxine despite 5% water in DMF (polymerization solvent). Given the similarities in monomer performance in solution, the same conditions were employed for the dispersion polymerization of 3-BAEPhA (20 wt/vol%) as for 3-BAPhA (above), although the medium was different (1 : 2 water/EtOH as opposed to 3 : 1 water/EtOH). The greater proportion of ethanol allowed solvation of the more hydrophobic monomer 3-BAEPhA, while maintaining insolubility of the derived polymer. Since heterogeneous polymerizations of BBMA over longer polymerization times have been reported to give a slight coagulum,[7] the short polymerization time of 2 h was expected to minimise pinacol group hydrolysis and boroxine formation. Using the longer steric stabiliser poly(DMA)$_{96}$ macroRAFT agent with 3-BAEPhA (20 wt/vol%) for targeted degree of polymerizations (DPs) = 50, 150 and 200 (Fig. 3) resulted in shifts in M_n to higher MWs of (M_n=) 20 700, 39 000, and 44 500 g mol^{-1} respectively, at near-full (99%) conversion (Run 5–7, Table 1). The low MW tail contributes to the high $Đ$ = 1.57–1.76, and is consistent with the carryover of dead chains from the preparation of the poly(DMA)$_{96}$ (M_n = 9900 g mol^{-1}, $Đ$ = 1.17) by chain extension of poly(DMA)$_{39}$ (M_n = 4200 g mol^{-1}, $Đ$ = 1.10) (Fig. S10,† thus polyDMA)$_{96}$ is equiv. to poly(DMA)$_{39}$-*b*-poly(DMA)$_{57}$). Note attempted preparation of this longer stabilizer block in a single RAFT polymerization of DMA at 70 °C with [DMA]$_0$/[DMP]$_0$ = 100, resulted in lower conversion (72%) and thus shorter stabilizer, poly (DMA)$_{65}$ (M_n = 6800 gmol^{-1}, $Đ$ = 1.15) (Fig. S11†). However, dead chains (in Fig. 3(a)) are also due to the increasing [VA-044]$_0$ used with higher targeted DP. The appearance of the resulting polymerization mixtures was gel-like, but importantly with no brown coagulum (Fig. 3). The lowest DP sample gave the only non-cloudy gel, with viscosity appearing to decrease with increasing DP. In PISA, the formation of worm-like micelles is often the cause of increases in viscosity due to worm entanglement.[22] Long worms of up to 1 μm in length are evident at the lowest targeted DP along with interconnected spherical particles (Run 5). Support for the decrease in

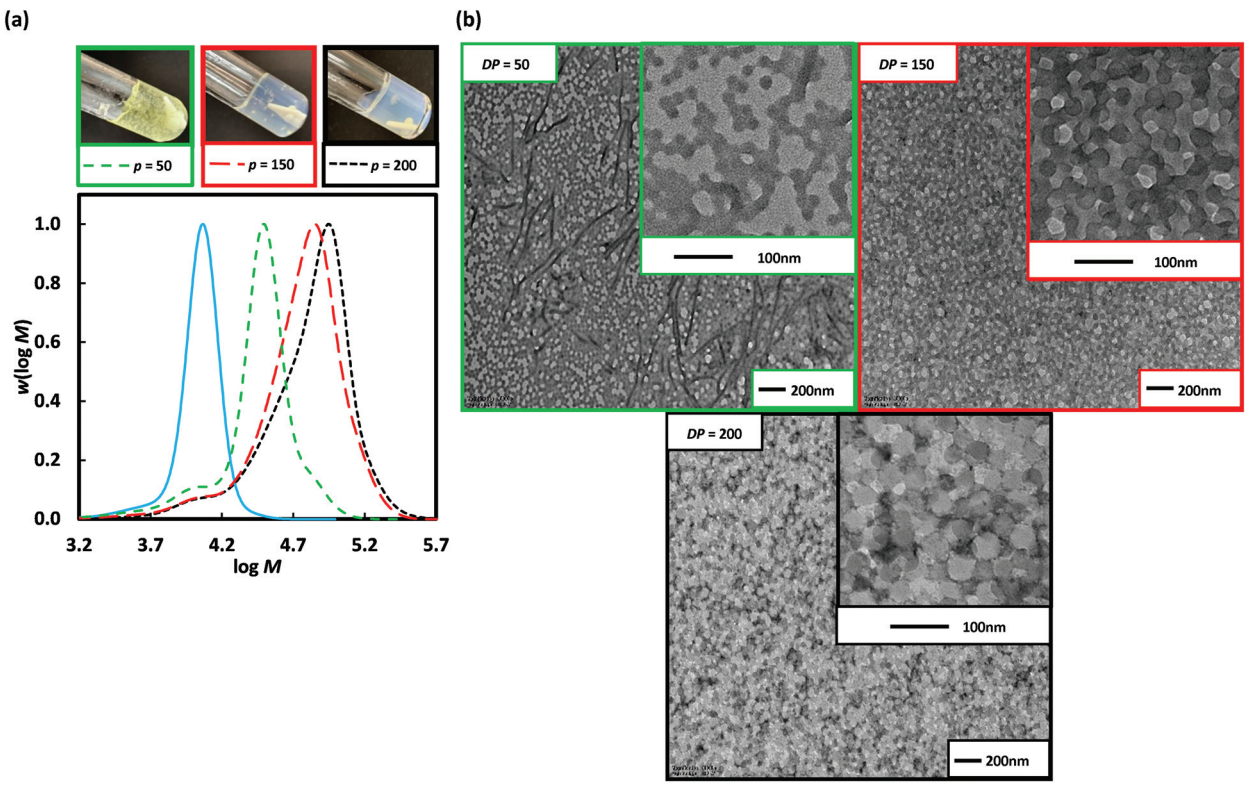

Fig. 3 Poly(DMA)$_{96}$ as macroRAFT agent (solid blue line) in the 2 h dispersion polymerizations of 3-BAEPhA (20 wt/vol%) in 1 : 2 water/EtOH at 70 °C, where [poly(DMA)$_{96}$]$_0$/[VA-044]$_0$ = 50, 20, 14 for targeted degree of polymerization, DP = 50 (Run 5), 150 (Run 6) and 200 (Run 7) respectively. (a) Visual appearance of polymerizations (with white stirrer bar within) and MWDs (99% conv.); (b) TEM images for PISA (additional images in Fig. S7–S9,† respectively).

Open Access Article. Published on 07 June 2022. Downloaded on 12/30/2025 1:10:31 PM.
This article is licensed under a Creative Commons Attribution 3.0 Unported Licence.

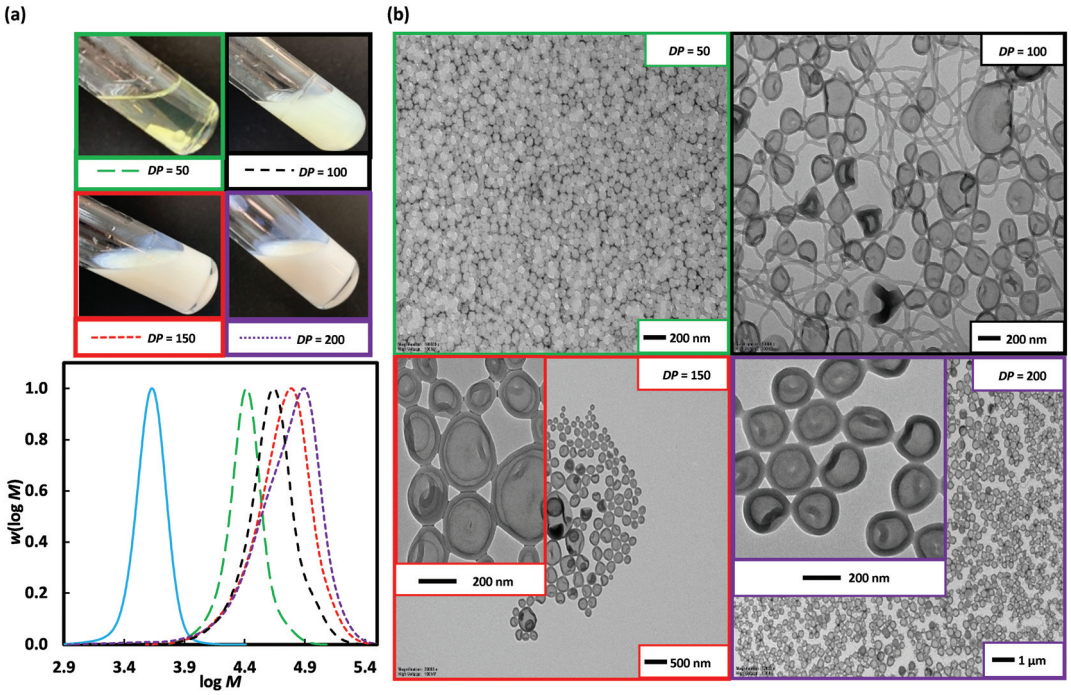

Fig. 4 Poly(DMA)$_{36}$, as macroRAFT agent (solid blue line) in the 2 h dispersion polymerizations of 3-BAEPhA (20 wt/vol%) in 1 : 2 water/EtOH at 70 °C, where [poly(DMA)$_{36}$]$_0$/[VA-044]$_0$ = 50, 25, 17 and 12 for targeted degree of polymerization, DP = 50 (Run 8), 100 (Run 9), 150 (Run 10) and 200 (Run 11) respectively. (a) Visual appearance of polymerizations (with white stirrer bar within) and MWDs (99% conv.); (b) TEM images for PISA (additional images in Fig. S12–S15,† respectively).

viscosity is the replacement of the worm-like micelle phase at the lowest DP with about 20 nm solid NPs at DP = 150 (Run 6) and 200 (Run 7) (Fig. 3). From Run 6 to 7, the M_n(GPC) increase of 5,500 g mol^{-1} surprisingly resulted in little effect on morphology, other than rounder NPs.

The particle morphology in PISA is primarily dictated by the relative volume fractions of the two blocks as described by the packing parameter (P).[5] Thus, extending a shorter stabiliser macroRAFT agent allows easier access to a wider range of morphologies. Poly(DMA)$_{36}$ (as opposed to poly(DMA)$_{96}$ above) was used for 2 h dispersion polymerization of 3-BAEPhA (20 wt/vol%) using targeted DP of 50 (Run 8), 100 (Run 9), 150 (Run 10), and 200 (Run 11) at 70 °C (Fig. 4). Free-flowing white stable colloidal dispersions were formed for all polymerizations, apart from at the highest initial poly(DMA)$_{36}$ concentration (DP = 50), which resulted in a clear gel. All polymerizations proceeded to completion (99%) in the case of DP = 50, 100, and 150, with narrow MWDs ($Đ$ = 1.15–1.38), with only the MWD at DP = 200 ($Đ$ = 1.63, Table 1) broad. High blocking efficiency was indicated by M_n of 23 600, 30 500, and 43 100 g mol^{-1} in relatively close agreement with $M_{n,th}$ of 17 600, 30 900, and 44 600 g mol^{-1} for targeted DP = 50, 100, and 150 respectively. For DP = 50 (Run 8), ~10 nm solid spherical particles of narrow size distribution were obtained (Fig. 4), with TEMs showing similar morphology to Runs 6 and 7 (DP = 150 and 200 from poly(DMA)$_{96}$), indicative of similar P or comparable ratios of solvophilic (poly(DMA)) to solvophobic (poly(3-BAEPhA)) chain lengths. The size of polymer objects significantly increases from DP = 50 to DP = 100, with 50–200 nm diameter vesicles with filaments/worms within aggregates evident in the TEM images of Run 9. For DP = 150 (Run 10), there are no worms, with 50–300 nm diameter spherical vesicles observed. Increasing DP further (DP = 200, Run 11) yields a narrower distribution of vesicles of mostly 200 nm in diameter. In TEM images for Run 9–11 encapsulation of NPs within vesicles is apparent, with at the highest DP, most particles appearing as yolk–shell type vesicles.[23]

In summary, PISA is successful for the unprotected BA monomer (3-BAPhA) when using a longer stabilizer poly(DMA) block, yielding mainly spherical NPs. This polymerization appears to proceed in two phases giving boroxine agglomeration and a separable free-flowing dispersion. These suspended NPs undergo room temperature morphology transitions by aqueous dilution, where hydrolysis of the boroxine core to BA occurs. This new type of stimuli-responsive NP will be the subject of future investigations with the free BA moieties allowing sugar-sensing. Pinacol group protection (in 3-BAEPhA) prevents boroxine formation, with PISA giving core–shell spherical polyacrylamide NPs and an array of higher order objects, including worms and vesicles.

Author contributions

H.S.D. experimentation, methodology and writing; F.I. experimentation and methodology (TEM); A.E. supervision; P.B.Z.

 This journal is © The Royal Society of Chemistry 2022

and F.A. conceptualization, supervision, writing-review, and editing. All authors have given approval to the final version of the manuscript.

Conflicts of interest

The authors declare no competing financial interest.

Notes and references

1 X. Sun and T. D. James, *Chem. Rev.*, 2015, **115**, 8001–8037.
2 W. L. A. Brooks and B. S. Sumerlin, *Chem. Rev.*, 2016, **116**, 1375–1397.
3 N. J. Penfold, W. J. Yeow, C. Boyer and S. P. Armes, *ACS Macro Lett.*, 2019, **8**, 1029–1054.
4 D. Le, D. Keller and G. Delaittre, *Macromol. Rapid Commun.*, 2019, **40**, 1800551.
5 N. J. Warren and S. P. Armes, *J. Am. Chem. Soc.*, 2014, **136**, 10174–10185.
6 F. D'Agosto, J. Rieger and M. Lansalot, *Angew. Chem., Int. Ed.*, 2020, **59**, 8368–8392.
7 L.-C. S. Huang, D. Le, I.-L. Hsiao, S. Fritsch-Decker, C. Hald, S.-C. Huang, J.-K. Chen, J. R. Hwu, C. Weiss, M.-H. Hsu and G. Delaittre, *Polym. Chem.*, 2021, **12**, 50–56.
8 B. Fan, J. Wan, J. Zhai, X. Chen and S. H. Thang, *ACS Nano*, 2021, **15**, 4688–4698.
9 A. Pitto-Barry, *Polym. Chem.*, 2021, **12**, 2035–2044.
10 D. Roy, J. N. Cambre and B. S. Sumerlin, *Chem. Commun.*, 2008, 2477–2479.
11 D. Roy, J. N. Cambre and B. S. Sumerlin, *Chem. Commun.*, 2009, 2106–2108.
12 J. N. Cambre, D. Roy and B. S. Sumerlin, *J. Polym. Sci., Part A: Polym. Chem.*, 2012, **50**, 3373–3382.
13 J. Zou, S. Zhang, R. Shrestha, K. Seetho, C. L. Donley and K. L. Wooley, *Polym. Chem.*, 2012, **3**, 3146–3156.
14 S.-S. Li, X.-H. Lv, X.-L. Sun, W.-M. Wan and H. Bao, *Polym. Chem.*, 2020, **11**, 2914–2922.
15 L. Zhang and A. Eisenberg, *Science*, 1995, **268**, 1728–1731.
16 G. Gody, T. Maschmeyer, P. B. Zetterlund and S. Perrier, *Macromolecules*, 2014, **47**, 3451–3460.
17 B. A. Chalmers, A. Alzahrani, G. Hawkins and F. Aldabbagh, *J. Polym. Sci., Part A: Polym. Chem.*, 2017, **55**, 2123–2128.
18 P. B. Zetterlund, Y. Kagawa and M. Okubo, *Chem. Rev.*, 2008, **108**, 3747–3794.
19 A. Blanazs, J. Madsen, G. Battaglia, A. J. Ryan and S. P. Armes, *J. Am. Chem. Soc.*, 2011, **133**, 16581–16587.
20 A. L. Korich and P. M. Iovine, *Dalton Trans.*, 2010, **39**, 1423–1431.
21 S. E. Burke and A. Eisenberg, *Langmuir*, 2001, **17**, 6705–6714.
22 L. A. Fielding, J. A. Lane, M. J. Derry, O. O. Mykhaylyk and S. P. Armes, *J. Am. Chem. Soc.*, 2014, **136**, 5790–5798.
23 W.-M. Wan and C.-Y. Pan, *Macromolecules*, 2010, **43**, 2672–2675.

Open Access Article. Published on 07 June 2022. Downloaded on 12/30/2025 1:10:31 PM.
This article is licensed under a Creative Commons Attribution 3.0 Unported Licence.